Channel Correlation Relied Grouped Spatial Modulation for Massive MIMO Systems

Xingxuan Zuo[1], *Jiankang Zhang*[2],*Xiaomin Mu*[1],*Lie-Liang Yang*[2]

[1] *School of Information Engineering, Zhengzhou University, 450001, Zhengzhou, China*
[2] *School of Electronics and Computer Science, University of Southampton, SO17 1BJ, Southampton, UK*
** E-mail: lly@ecs.soton.ac.uk*

Abstract: Massive multiple input multiple output (MIMO) systems with hundreds of correlated antennas at base station (BS) are capable of offering abundant spatial resources. When spatial-domain modulation is applied to these systems, the spatial modulation (SM) [1] using only one radio frequency (RF) chain benefits practical implementation, but suffers from significantly reduced multiplexing gain offered by the massive number of antennas. By contrast, the generalized spatial modulation (GSM) [2] allows to simultaneously activate multiple transmit antennas, which improves spatial multiplexing gain, but degrades the achievable error performance, as its design pays no attention to the antenna correlation. In this paper, we propose an antenna grouped spatial modulation (GrSM) scheme, which is capable of circumventing the shortcomings of both the SM and GSM schemes suffered in massive MIMO scenarios. In the proposed GrSM scheme, transmit antennas are partitioned into multiple groups, where the relatively strongly correlated antennas within individual groups are used to implement component SM schemes, while the relatively weakly correlated antennas in different groups are beneficial to obtain multiplexing gain. In order to further improve the spectral efficiency, adaptive modulation (AM) is integrated with GrSM to form the adaptive GrSM (AGrSM). The achievable error and spectral efficiency performance of GrSM and AGrSM systems are investigated based on both mathematical analysis and Monte-Carlo simulations, which are also compared with that of the conventional SM and GSM schemes, when massive MIMO communication scenarios are considered. Our studies and performance results show that GrSM is a promising transmit scheme for massive MIMO, which can outperform both the SM and GSM schemes.

1 Introduction

Massive multiple input multiple output (MIMO) [3], which has the potential to achieve high spectral and energy efficiency, has been considered as one of the promising techniques for the fifth generation (5G) wireless communications [4]. This is because massive MIMO systems are capable of offering abundant spatial resources, which may be exploited for different purposes. Among them, spatial modulation (SM) [1] can exploit the spatial resources in massive MIMO for conveying extra bits using space shift keying (SSK) modulation. Specifically, by activating a single transmit antenna at each time slot, SM has the advantages of single radio-frequency (RF) chain, avoiding inter channel interference (ICI) and of mitigating the problem of inter antenna synchronization (IAS) [5]. In addition to SSK, SM also transmits an amplitude/phase modulation (APM) using the activated antenna to convey information. Hence, a SM conveys information in both the signal domain and the spatial domain [6]. However, a limitation of SM is that the data rate contributed by the spatial domain is proportional to the *logarithm* of the number of transmit-antennas. When operated with the massive MIMO systems where a huge number of transmit antennas is available, this SM scheme becomes less efficient, yielding low spectral efficiency [7].

In order to improve the spectral efficiency of SM, generalised spatial modulation (GSM) has been proposed and investigated, e.g., in [2], which allows several transmit antennas to be simultaneously activated for conveying information in both the space domain and the signal domain[8]. In [9], the authors have proposed a low complexity detection algorithm for GSM systems based on the message passing principles. The comparison between SM and GSM has been carried out, e.g., in [10], showing that GSM is capable of improving the spectral efficiency of SM, while suffers from the degradation of bit error rate (BER) performance due to the existence of multiple active antennas.

It is well known that the performance of spatial multiplexing in MIMO degrades significantly with the increase of spatial correlation [11, 12]. In order to mitigate the effect of spatial correlation, various antenna grouping techniques have been proposed and investigated via combining transmit beamforming and spatial multiplexing [13–15]. It can be shown that antenna grouping is an effective strategy for alleviating the loss of the multiplexing gain resulted from antenna correlation. In [16], different grouping schemes have been introduced based on different criteria, which also result in different error performance, spectrum efficiency and energy efficiency. In [17], a grouping assisted GSM has been proposed, which divides the transmit antennas into several groups either by selecting adjacent antennas for a group, forming the block grouping, or by maximizing the antenna distance in one group, yielding the interleaved grouping. However, the two grouping methods in [17] are based on the statistical channel information, which can be improved when the knowledge of real time channel correlation is available.

On the other side, when time-varying channel knowledge is available to BS transmitter, the BS may implement adaptive resource allocation via changing its transmission parameters, such as, power level, modulation level, coding rate, spectrum band, etc., in order to maximise the achievable rate [18, 19]. Specifically, with the aid of channel knowledge, adaptive modulation (AM) schemes can improve the transmission data rate at a given BER requirement via adapting the constellation size according to channel states [20]. Owing to this merit, by invoking adaptive modulation, the adaptive SM (ASM) and adaptive GSM (AGSM) have been proposed to further improve the spectrum-efficiency in SM [21, 22].

Against the background and inspired by the existing research results, in this paper, we propose a grouped spatial modulation (GrSM) scheme, where antennas are grouped with the aid of the information about the instantaneous channel correlation. Within each of the groups, the SM is independently implemented by activating one transmit antenna per time slot, and hence, multiplexing transmission is operated across different groups. By activating multiple transmit antennas experiencing the fading of relatively low correlation, our proposed GrSM has the merit to overcome the limitation imposed by the spatial dimension. Furthermore, it is capable of mitigating the performance loss due to antenna correlation, as argued in Section 3. In this paper, we analyse the performance of GrSM systems by deriving an upper bound for the average bit error

rate (ABER), which is shown to be tight at moderate to high signal to noise ratio (SNR). We also analyse the sum-rate of GrSM systems. Furthermore, we introduce AM to our GrSM, forming the AGrSM, in order to further improve its spectral efficiency. Finally, via simulation and numerical methods, we compare the proposed GrSM scheme with some existing schemes in terms of the BER and sum-rate performance. Our studies and performance results show that the proposed GrSM outperforms the SM, and also outperforms the existing GSM schemes.

In summary, the main contribution and novelty of this paper can be summarized as follows:

- A novel GrSM scheme is proposed, in which transmit antennas are grouped with the aid of the *instantaneous* channel correlation information.
- The sum-rate and complexity of the proposed GrSM are analysed. Moreover, AM is introduced to the GrSM, to form a AGrSM scheme, in order to achieve the highest possible data rate.
- The BER, sum-rate, and spectral efficiency performance of the proposed GrSM and AGrSM are investigated based on Monte-Carlo simulations and our analytical results. The BER and spectral efficiency performance of GrSM and AGrSM are also compared with the existing GSM, SM, and AGSM schemes.

The remainder of the paper is structured as follows. In Section 2, we first consider the system model. Then, the achievable sum-rate of GrSM and adaptive rate transmission in GrSM systems are addressed. The principle of antenna grouping is detailed in Section 3. In Section 4, we analyse the BER and spectral efficiency performance of GrSM and AGrSM systems. Performance results are demonstrated and discussed in Section 5, and finally, Section 6 provides a summary of the main contributions of the paper.

2 System Model, Sum-Rate and Adaptive Rate Transmission

2.1 Grouped Spatial Modulation

The system model for the proposed GrSM scheme operated in massive MIMO scenarios consists of a transmitter having N_t transmit antennas, and a receiver with $N \geq 1$ receive antennas, where N_t is on the order of tens to even hundreds of N. We assume that the GrSM massive MIMO system is operated in the time-division duplex (TDD) mode. Hence, the channel state information (CSI) for the transmitter-receiver channels can be obtained via the channel estimation of the receiver-transmitter channels [23, 24]. In our GrSM system, specially, the N_t transmit antennas are partitioned into $K(K \geq N)$ groups based on the instantaneous knowledge about antenna correlation, as detailed in Section 3. Within each of the K groups, only one antenna is activated to transmit one APM symbol concurrently. Hence, there are in total K SSK symbols and K APM symbols transmitted per GrSM symbol period.

We assume that both the receiver and the transmitter know the channel state information. The total N_t transmit antennas are assumed to be equally divided into K groups. Hence, each group has $N_g = N_t/K$ antennas. We also assume that all antennas have an equal probability to be activated. Since each group activates one transmit antenna during one symbol period, the number of antenna activation patterns in one group is N_g, and the total number of antenna activation patterns in the GrSM system is $(N_g)^K$. Consequently, $\lfloor K \log_2 N_g \rfloor$ bits per symbol can be delivered by the antenna patterns, where $\lfloor . \rfloor$ is a floor operation. When both SSK and M-ary APM symbols are considered, the total number of bits conveyed per GrSM symbol is given by the formula

$$\eta_{\text{Gr}} = \lfloor K \log_2 N_g \rfloor + K \log_2 M \tag{1}$$

By contrast, when the GSM [9] is implemented to activate K out of N_t transmit antennas for transmitting K number of M-ary APM symbols, the total number of bits per symbol is

$$\eta_{\text{GSM}} = \left\lfloor \log_2 \binom{N_t}{K} \right\rfloor + K \log_2 M \tag{2}$$

where $\left\lfloor \log_2 \binom{N_t}{K} \right\rfloor$ is the number of bits delivered per symbol in the spatial domain. In comparison with GSM, the proposed GrSM scheme suffers from some data rate loss in the spatial domain, due to the fact that $\left\lfloor \log_2 \binom{N_t}{K} \right\rfloor \geq \lfloor K \log_2 N_g \rfloor$. However, for compensation, higher order APM modulation can be employed in GrSM to attain a similar spectral efficiency. This guarantees that GrSM scheme is capable of achieving a higher spectrum-efficiency than GSM scheme, as demonstrated in Section 5.

2.2 Modelling of Received Signal

Let x_k and s_k represent the APM symbol and SSK symbol transmitted by the k-th group during a symbol period. Then, at the receiver, we have the N-length observation vector of

$$\boldsymbol{y} = \sum_{k=1}^{K} \boldsymbol{H}_k \boldsymbol{e}_{s_k} x_k + \boldsymbol{w} \tag{3}$$

where $\boldsymbol{H}_k \in \mathbb{C}^{N \times N_g}$ is the channel matrix relating the k-th group of transmit antennas to the N receive antennas. In many practical wireless communication scenarios where the transmit distance is relatively short, there may exist line of sight (LOS) propagation paths. Hence, in this contribution, we assume the Rician fading channel model. In Eq. (3), $\boldsymbol{e}_{s_k}$ represents the s_k-th column of $\boldsymbol{I}_{N_g}$ of the N_g-dimensional identity matrix. Furthermore, $\boldsymbol{w}$ is a N-length complex Gaussian noise vector distributed with zero mean and a covariance matrix of $\sigma_w^2 \boldsymbol{I}_N$.

Let $\boldsymbol{H} = [\boldsymbol{H}_1, \boldsymbol{H}_2, \cdots, \boldsymbol{H}_K]$. Then, we can rewrite Eq. (3) as

$$\boldsymbol{y} = \boldsymbol{H}\boldsymbol{x} + \boldsymbol{w} \tag{4}$$

where $\boldsymbol{x} = [\boldsymbol{e}_{s_1}^T x_1, \boldsymbol{e}_{s_2}^T x_2, \cdots, \boldsymbol{e}_{s_K}^T x_K]^T$ and is in a form of

$$\boldsymbol{x} = [\underbrace{0, 0, \cdots, x_1, \cdots, 0}_{N_g}, \underbrace{0, x_2, 0, \cdots, 0}_{N_g}, \cdots, \underbrace{0, \cdots, 0, x_K}_{N_g}]^T \tag{5}$$

As seen in $\boldsymbol{x}$, each group corresponds to N_g transmit antennas. Specifically within the k-th group, one of the N_g transmit antennas is activated by the SSK symbol s_k to transmit an APM symbol x_k.

2.3 Channel Modelling

When there is correlation existing among transmit antennas and/or among receive antennas, the Kronecker model [25] is usually utilized to model the spatial correlation (SC) of the scattering components. According to [26], the scattering components of the MIMO spatial channel can be expressed as

$$\boldsymbol{H} = \boldsymbol{R}_{\text{rx}}^{\frac{1}{2}} \tilde{\boldsymbol{H}} \boldsymbol{R}_{\text{tx}}^{\frac{1}{2}} \tag{6}$$

where $\tilde{\boldsymbol{H}}$ is uncorrelated channel, has i.i.d. complex entries and each of them has the distribution $\mathcal{CN}(0, 1)$, denoting a complex Gaussian distribution with mean zero and variance 1. $\boldsymbol{R}_{\text{tx}}$ and $\boldsymbol{R}_{\text{rx}}$ are the correlation matrices of transmitter and receiver antennas, respectively. In our study, we adopt the exponential correlation model [**?**].

Correspondingly, $\boldsymbol{R}_{\text{tx}}$ and $\boldsymbol{R}_{\text{rx}}$ are can be expressed in the form of

$$\boldsymbol{R} = \begin{bmatrix} 1 & \rho & \rho^2 & \cdots & \rho^{n-1} \\ \vdots & \ddots & \ddots & \ddots & \vdots \\ \rho^{n-1} & \cdots & \rho^2 & \rho & 1 \end{bmatrix} \tag{7}$$

where $\rho = \exp(-\beta)$ with β being the correlation coefficient between two adjacent transmit (or receive) antennas, while $n = N_t$ or N.

2.4 Achievable Sum-Rate

The number of bits conveyed per symbol by the GrSM scheme includes both that conveyed by the APM and that by the SSK. Hence, the total sum-rate per symbol is [27],

$$R_{GrSM} = R_{signal} + R_{spatial} \tag{8}$$

where R_{signal} and $R_{spatial}$ represent the rate supportable by the signal domain and that by the spatial domain, respectively.

Let us assume that the transmit power is normalized to unit, meaning that $E_s = E[\|\boldsymbol{x}\|^2] = 1$. Then, the first term of Eq. (8) represents the rate achievable by the APM. When given an antenna pattern, e.g., the i-th antenna pattern, the GrSM system is reduced to a MIMO system with K transmit antennas and N receive antennas, which for a given $\boldsymbol{H}$ has the achievable rate of [28, 29]

$$R(\boldsymbol{H}, i) = \log_2 \left[\det \left(\boldsymbol{I}_N + \frac{\boldsymbol{H}(i)\boldsymbol{H}^{\text{H}}(i)}{N\sigma_w^2} \right) \right] \tag{9}$$

where index i means the i-th antenna pattern, and $\boldsymbol{H}(i)$ is the $(N \times K)$ channel matrix obtained from $\boldsymbol{H}$ according to the i-th antenna pattern. After taking all antenna patterns and channel statistics into account, the ergodic rate achievable by the APM can then be expressed as

$$R_{signal} = E_{\boldsymbol{H}} \left\{ \frac{1}{|\mathcal{A}|} \sum_{i \in \mathcal{A}} R(\boldsymbol{H}, i) \right\} \tag{10}$$

where the expectation is taken with respect to the statistics of $\boldsymbol{H}$, and $\mathcal{A}$ is a set containing all the antenna patterns exploited by GrSM.

Let us assume that $x_k, k = 1, \cdots, K$, are independent and obey the same complex Gaussian distribution, expressed as $x_k \sim CN(0, \sigma_x^2 = 1/K)$. Then, the probability density function (PDF) of $\boldsymbol{x}$ can be expressed as

$$p(\boldsymbol{x}) = \prod_{k=1}^{K} p(x_k) = \frac{1}{(\pi\sigma_x^2)^K} \exp \left[-\sum_{k=1}^{K} \frac{|x_k|^2}{\sigma_x^2} \right] \tag{11}$$

where $|\cdot|$ denotes the modulus operator.

Consequently, the PDF of the received observations on the condition that the i-th, $i \in \mathcal{A}$, antenna pattern is activated can be written as

$$\begin{aligned} p(\boldsymbol{y}|i \in \mathcal{A}) &= \frac{1}{\pi^N \det(\boldsymbol{R}_{y|i})} \exp(-\boldsymbol{y}^{\text{H}} \boldsymbol{R}_{y|i}^{-1} \boldsymbol{y}) \\ &= \frac{1}{\pi^N \det(\boldsymbol{H}(i)\boldsymbol{C}_x\boldsymbol{H}^H(i) + \sigma_w^2 \boldsymbol{I}_N)} \\ &\times \exp\left(-\boldsymbol{y}^H (\boldsymbol{H}(i)\boldsymbol{C}_x\boldsymbol{H}^H(i) + \sigma_w^2 \boldsymbol{I}_N)^{-1} \boldsymbol{y} \right) \end{aligned} \tag{12}$$

where $\boldsymbol{R}_{y|i}$ is the autocorrelation matrix of $\boldsymbol{y}$ when given the i-th activation pattern, and $\boldsymbol{C}_x$ is the covariance matrix of $\boldsymbol{x}$, given by $\boldsymbol{C}_x = \boldsymbol{I}_{\boldsymbol{K}}/K$.

Hence, the rate $R_{spatial}$ in Eq. (8) can be evaluated from the formula of [27]

$$\begin{aligned} R_{spatial} &= \max I(i \in \mathcal{A}; \boldsymbol{y}) \\ &= \max_{p(i)} \int \left[\sum p(i) p(\boldsymbol{y}|i) \log_2 \left(\frac{p(\boldsymbol{y}|i)}{p(\boldsymbol{y})} \right) d\boldsymbol{y} \right] \\ &= \frac{1}{|\mathcal{A}|} \sum_{i \in \mathcal{A}} \left[\int_{\boldsymbol{y}} p(\boldsymbol{y}|i) \log_2 \frac{p(\boldsymbol{y}|i)}{p(\boldsymbol{y})} d\boldsymbol{y} \right] \end{aligned} \tag{13}$$

where $p(i)$ denotes the probability of selecting the i-th antenna pattern, which is assumed to be uniform. Hence, we have $p(i) = 1/|\mathcal{A}|$. In (13), $p(\boldsymbol{y}) = \sum_{i \in \mathcal{A}} p(i) p(\boldsymbol{y}|i)$.

2.5 Adaptive Rate Transmission

Since channels are time-variant, transmission with adaptive rate and power-control is required to achieve the data rate as high as possible. In this paper, for simplicity, we consider constant-power but variable-rate M-ary QAM (M-QAM) for information transmission. For achieving this, the SNR range is divided into $N_a - 1$ subregions, which are defined by the switching thresholds $\{\gamma_n\}_{n=1}^{n=N_a}$. Correspondingly, a constellation size M_n is assigned to the n-th subregion. Specifically, when the received SNR γ_r is estimated to be in the n-th region, namely $\gamma_n \leq \gamma_r < \gamma_{n+1}$, where by definition, $\gamma_{N_a} \to \infty$, the QAM constellation of size M_n is utilized to transmit at the rate of $\log_2 M_n$.

The switching boundaries can be set based on the BER of the QAM schemes employed. Specifically, when a M_n-QAM is operated at the SNR of γ, the BER is that over additive white Gaussian noise (AWGN) channel, which is given by [30]

$$P_{b_n}(\gamma) = \frac{1}{5} \exp \left[\frac{-3\gamma}{2(M_n - 1)} \right] \tag{14}$$

Then, when given a target BER of P_{b_0}, the region boundaries, namely the switching thresholds γ_n for $n = 1, 2, \cdots, N_a - 1$ can be derived to be

$$\gamma_n = -\frac{2}{3} \ln(5P_{b_0})(M_n - 1) \quad n = 1, 2, \cdots, N_a - 1 \tag{15}$$

3 Antenna Grouping

Since transmit (also receive) antennas are correlated, dividing different antennas into different groups may generate different performance. Based on the channel's correlation matrix, our antenna grouping in this paper is designed to maximize the achievable rate. Let us represent the channel correlation matrix as

$$\boldsymbol{M} = \begin{bmatrix} 1 & M_{1,2} & \cdots & M_{1,N_t} \\ M_{2,1} & 1 & \cdots & M_{2,N_t} \\ \vdots & \vdots & \ddots & \vdots \\ M_{N_t,1} & M_{N_t,2} & \cdots & 1 \end{bmatrix} \tag{16}$$

where the (i, j)-th element is given by [31]

$$M_{i,j} = \frac{1}{\|\boldsymbol{h}_i\| \cdot \|\boldsymbol{h}_j\|} \cdot [\boldsymbol{H}^H \boldsymbol{H}]_{ij} \tag{17}$$

In Eq. (17), $\boldsymbol{h}_i$ denotes the i-th column of $\boldsymbol{H}$, which contains the channels from the i-th transmit antenna to all the N receive antennas. Therefore, $M_{i,j}$ represents the correlation coefficient between the channels from the i-th transmit antenna and that from the j-th transmit antenna. Furthermore, it can be shown that, in (16), we have $M_{i,j} = M_{j,i}^*$.

It is well-known that a bigger value of $|M_{i,j}|$ implies a stronger correlation between $\boldsymbol{h}_i$ and $\boldsymbol{h}_j$. The spatial multiplexing gain of a

MIMO system degrades as the antenna correlation increases, or as the values of $|M_{i,j}|$ for different (i,j) increase [16]. Hence, based on the antenna correlation matrix of Eq. (16) and with the motivation to achieve a sum-rate as high as possible, the N_t transmit antennas should be partitioned into K disjoint groups as follows. Given the N_t channel vectors $\boldsymbol{h}_i$ and the corresponding channel correlation matrix of Eq. (16), the N_t transmit antennas are assigned to the K groups, by allowing the N_g transmit antennas assigned to the same group to have the correlation as high as possible, while simultaneously the transmit antennas assigned to different groups have the correlation as low as possible. In this way, the sum-rate of the massive MIMO system can be improved. This is because on one side, the spatial multiplexing gain achieved relying on the transmit antennas across different groups can be maximized. On the other side, the performance of the SSK designed based on the N_g transmit antennas within one group may not be significantly affected [24]. The reason behind this statement is that although the antennas in one group are possibly highly correlated, the signals received from them are generally different, and hence can be efficiently distinguished with the aid of the maximum likelihood (ML) detection. For example in the extreme case when the signals from a group of transmit antennas experience the same fading, making the transmit antennas of one group act like a phase-shifting antenna array, the SSK signal can also be detected by the ML detection in the principles of phase-shift keying modulation [32].

In summary, the proposed antenna grouping algorithm is stated as Algorithm 1, which implements what we considered above. Given the numbers of N_t, K, and hence $N_g = N_t/K$, we can readily figure out that the total number of combinations for dividing N_t transmit antennas into K groups is given by

$$N_D = \prod_{n=0}^{K-1} \binom{N_t - nN_g - 1}{N_g - 1} = \frac{1}{K!} \prod_{n=0}^{K-1} \binom{N_t - nN_g}{N_g} \quad (18)$$

The objective of Algorithm 1 is to find the best combination from these N_D combinations.

Algorithm 1. *(***Antenna Grouping Algorithm***):*

1) Input: N_t, K, N_g, $\boldsymbol{H}$.
Initialization: Compute $\boldsymbol{M}$ using (17)*, and prepare the N_D combinations of candidate groupings.*
2) For each combination of $1 \le m \le N_D$, calculate

$$R_m = \sum_{k=1}^{K} \sum_{i=1}^{N_g-1} \sum_{j=i+1, j\neq i}^{N_g} |M_{i,j}^{(k)}| \quad (19)$$

where $M_{i,j}^{(k)}$ is the correlation coefficient between the channels from the i-th transmit antenna of the k-th group and the channels from the j-th transmit antenna of the k-th group.
3) Determine the winning combination as

$$\hat{m} = \arg \max_{m=1,\ldots,N_D} R_m \quad (20)$$

and the final K groups of transmit antennas can be obtained from the $\hat{m}$-th combination.

The complexity of the above antenna grouping algorithm can be analysed as follows. As the algorithm needs to compute $\boldsymbol{M}$ of Eq. (16) using Eq. (17), compute N_D number of R_m using Eq. (19), and find the maximum of R_m based on Eq. (20), we analyse the complexity of the algorithm by analysing these terms in detail. First, to compute the channel correlation matrix $\boldsymbol{M}$, it needs to compute $\boldsymbol{H}^H\boldsymbol{H}$ once, which requires $N_t^2 N$ complex multiplications and $N_t^2(N-1)$ complex additions; and to compute the norms of the N_t columns of $\boldsymbol{H}$ once, which needs $N_t N$ complex multiplications and $N_t(N-1)$ real additions. With these at hand, forming M only needs about $N_t^2/2$ real multiplications and $N_t^2/2$ complex divisions due to $M_{i,j} = M_{j,i}^*$. For computing the N_D number of R_m, we can readily show that the total number of additions is upper-bounded by $N_D N_t N_g = N_D N_t^2/K$. Finally, finding the maximum among the N_D number of R_m requires $(N_D - 1)$ comparisons. When considering all the above computational requirements and ignoring the insignificant terms, it can be shown that the complexity of Algorithm 1 is $\mathcal{O}((N + N_D/K)N_t^2)$*.

4 Theoretical Analysis of BER and Spectral Efficiency

In this section, we analyse the performance of GrSM systems in terms of the BER and spectral efficiency, when different scenarios are considered.

4.1 Average Bit Error Rate

Following [33], the average BER of GrSM systems satisfies

$$\text{ABER} \le \frac{1}{2^{\eta_{Gr}}} \sum_{\{x_k, s_k\}} \sum_{\{\hat{x}_k, \hat{s}_k\}} \frac{N(\hat{\boldsymbol{x}}, \boldsymbol{x})}{\eta_{Gr}} E_{\boldsymbol{H}}\{P(\hat{\boldsymbol{x}}, \boldsymbol{x}|\boldsymbol{H})\} \quad (21)$$

where $N(\hat{\boldsymbol{x}}, \boldsymbol{x})$ is the number of bits in difference between $\hat{\boldsymbol{x}}$ and $\boldsymbol{x}$, $E_{\boldsymbol{H}}\{\cdot\}$ is the expectation with respect to the channel $\boldsymbol{H}$, η_{Gr} is the total number of bits conveyed per GrSM symbol, and $P(\hat{\boldsymbol{x}}, \boldsymbol{x}|\boldsymbol{H})$ represents the Pairwise Error Probability (PEP) conditioned on a given $\boldsymbol{H}$, which is given by [34–36]

$$\begin{aligned} P(\hat{\boldsymbol{x}}, \boldsymbol{x}|\boldsymbol{H}) =& P(\|\boldsymbol{y} - \boldsymbol{H}\hat{\boldsymbol{x}}\|^2 > \|\boldsymbol{y} - \boldsymbol{H}\boldsymbol{x}\|^2) \\ =& Q\left(\sqrt{\frac{\|\boldsymbol{H}(\hat{\boldsymbol{x}} - \boldsymbol{x})\|^2}{2\sigma_w^2}}\right) \end{aligned} \quad (22)$$

where $Q(x)$ is the Gaussian Q-function. Using its alternative representation of $Q(x) = \pi^{-1} \int_0^{\frac{\pi}{2}} \exp(-\frac{x^2}{2\sin^2\theta}) d\theta$, Eq. (22) can be rewritten as

$$P(\hat{\boldsymbol{x}}, \boldsymbol{x}|\boldsymbol{H}) = \frac{1}{\pi} \int_0^{\frac{\pi}{2}} \exp\left(-\frac{\varphi}{4\sigma_w^2 \sin^2\theta}\right) d\theta \quad (23)$$

where by definition, $\varphi = \|\boldsymbol{H}(\hat{\boldsymbol{x}} - \boldsymbol{x})\|^2$. Then, the expectation of Eq. (23) is given by

$$\begin{aligned} E_{\boldsymbol{H}}\{P(\hat{\boldsymbol{x}}, \boldsymbol{x}|\boldsymbol{H})\} =& \frac{1}{\pi} \int_0^{\frac{\pi}{2}} E\left[\exp\left(-\frac{\varphi}{4\sigma_w^2 \sin^2\theta}\right)\right] d\theta \\ =& \frac{1}{\pi} \int_0^{\frac{\pi}{2}} \int_0^{\infty} \exp\left(-\frac{\varphi}{4\sigma_w^2 \sin^2\theta}\right) f(\varphi) d\varphi d\theta \\ =& \frac{1}{\pi} \int_0^{\frac{\pi}{2}} M_{\varphi}\left(-\frac{1}{4\sigma_w^2 \sin^2\theta}\right) d\theta \end{aligned} \quad (24)$$

where $M_{\varphi}(\cdot)$ is the moment generating function (MGF) of φ [37]. According to [**?**], this MGF is given by

$$\begin{aligned} M_{\varphi}(s) =& \exp\left(s \times \boldsymbol{\mu}^H \boldsymbol{\Lambda}(\boldsymbol{I}_{KN_t} - s\boldsymbol{L}\boldsymbol{\Lambda})^{-1}\boldsymbol{\mu}\right) \\ & \times (\det[\boldsymbol{I} - s\boldsymbol{L}\boldsymbol{\Lambda}])^{-1} \end{aligned} \quad (25)$$

where $\boldsymbol{\Lambda} = \boldsymbol{I}_N \otimes (\hat{\boldsymbol{x}} - \boldsymbol{x})(\hat{\boldsymbol{x}} - \boldsymbol{x})^H$, $\boldsymbol{\mu} = \mu(\boldsymbol{I}_N \otimes \boldsymbol{R}_{\text{tx}})^{\frac{1}{2}} \times \boldsymbol{vec}(\mathbf{1}_{(N,N_t)})$ with μ being the mean of $\boldsymbol{H}$, $\boldsymbol{vec}(\cdot)$ being the vectorisation operator, $\mathbf{1}_{(N,N_t)}$ being a $(N \times N_t)$ all one matrix, and finally, $\boldsymbol{L} =$

As the convention, $\mathcal{O}(x)$ is defined as $\lim_{x\to\infty} \frac{\mathcal{O}(x)}{x} = c$, where c is a constant.

$\boldsymbol{I}_N \otimes \boldsymbol{R}_{\text{tx}}$ with $\otimes$ representing the Kronecker product. Upon substituting Eq. (25) into Eq. (24), finally, the average PEP as seen in Eq. (21) can be evaluated from the formula

$$E_{\boldsymbol{H}}\{P(\hat{\boldsymbol{x}},\boldsymbol{x}|\boldsymbol{H})\} = \frac{1}{\pi}\int_0^{\frac{\pi}{2}} \exp\left(-\frac{1}{4\sigma_w^2\sin^2\theta}\boldsymbol{\mu}^H\boldsymbol{\Lambda} \times \left[\boldsymbol{I}_{NN_t} + \frac{1}{4\sigma_w^2\sin^2\theta}\boldsymbol{L}\boldsymbol{\Lambda}\right]^{-1}\boldsymbol{\mu}\right) \times \left(\det\left[\boldsymbol{I}_{NN_t} + \frac{1}{4\sigma_w^2\sin^2\theta}\boldsymbol{L}\boldsymbol{\Lambda}\right]\right)^{-1} d\theta \tag{26}$$

4.2 Received SNR

For a GrSM system consisting of $(N_t \times N)$ antennas, the correlation among the transmit (or receive) antennas obeys the exponential profile. Considering that the number of active transmit antennas is K, according to [38], the probability density function (PDF) of the received SNR can be expressed as

$$f(\gamma) = \frac{\gamma^{\frac{(NK)^2}{r}-1}e^{-\frac{NK\gamma}{r\bar{\gamma}_a}}}{\Gamma(\frac{(NK)^2}{r})(\frac{r\bar{\gamma}_a}{NK})^{\frac{(NK)^2}{r}}} \tag{27}$$

where $r = NK + \frac{2\rho}{1-\rho}(NK - \frac{1-\rho^{NK}}{1-\rho})$ and $\bar{\gamma}_a = \frac{E[|h_{ij}|^2]}{\sigma_w^2}$ with h_{ij} being the (i,j)-th element of $\boldsymbol{H}$. From (27) the cumulative distribution function (CDF) of γ can be derived to be [32]

$$F(\gamma) = 1 - \sum_{k=0}^{\lfloor (NK)^2/r-1\rfloor} \frac{1}{k!}\left(\frac{NK}{r\bar{\gamma}_a}\right)^k e^{-\frac{NK\gamma}{r\bar{\gamma}_a}} \tag{28}$$

4.3 Spectral Efficiency

The average number of bits per symbol deliverable by the GrSM system is the sum of the number of bits per symbol transmitted in the spatial domain by the K groups, plus the average number of bits per symbol conveyed by the K APMs. Hence, the spectral efficiency of the GrSM system is

$$\eta_A = \lfloor K\log_2 N_g\rfloor + \eta_{APM} \text{ (bits per symbol)} \tag{29}$$

where η_{APM} is the total number of bits conveyed by the K APMs.

Following our analysis in Sections 2.5 and 4.2, when given the SNR boundaries of $\{\gamma_1,\gamma_2,\ldots,\gamma_{N_a}\}$ for implementation of adaptive modulations, and when given SNR's CDF of (28), the probability p_n of using the n-th modulation level with the constellation size M_n is given by

$$\begin{aligned} p_n =& P_r\left[\gamma_n \le \gamma_r < \gamma_{n+1}\right] \\ =& F(\gamma_{n+1}) - F(\gamma_n),\ n = 1,2,\ldots,N_a \end{aligned} \tag{30}$$

Therefore, the average number of bits per symbol conveyed by the K APMs is

$$\begin{aligned} \eta_{APM} =& K\sum_{n=1}^{N_a} p_n\log_2 M_n \\ =& K\sum_{n=1}^{N_a}\left(F(\gamma_{n+1}) - F(\gamma_n)\right)\log_2 M_n \end{aligned} \tag{31}$$

4.4 Average Bit Error Rate of Adaptive GrSM

An asymptotic BER bound for the AGrSM can be derived by following the approaches in [30, 35, 36, 39, 40]. Specifically, by following [40], the overall average BER of the AGrSM can be approximated as

$$P_e \approx P_a + P_d - P_aP_d \tag{32}$$

where P_a is the BER of the spatial domain information, on the condition that the APM symbols are correctly detected. According to [39], P_a can be evaluated from the formula

$$P_a \approx \frac{1}{2^\eta}\sum_{s_k}\sum_{\hat{s}_k}\frac{N(\hat{\boldsymbol{x}},\boldsymbol{x})}{\eta}E_{\boldsymbol{H}}\{P(\hat{\boldsymbol{x}},\boldsymbol{x}|\boldsymbol{H},\text{APMs})\} \tag{33}$$

where η is the number of bits transmitted by the spatial symbols, and $P(\hat{\boldsymbol{x}},\boldsymbol{x}|\boldsymbol{H},\text{APMs})$ is the conditional PEP between $\hat{\boldsymbol{x}}$ and $\boldsymbol{x}$ on the condition that the APM symbols are correct. The expectation of $P(\hat{\boldsymbol{x}},\boldsymbol{x}|\boldsymbol{H},\text{APMs})$ can be obtained from (26) by assuming that the APM symbols are correct, which can be shown to be

$$E_{\boldsymbol{H}}\{P(\hat{\boldsymbol{x}},\boldsymbol{x}|\boldsymbol{H},\text{APMs})\} = \frac{1}{\pi}\int_0^{\frac{\pi}{2}} \exp\left(-\frac{1}{4\sigma_w^2\sin^2\theta}\boldsymbol{\mu}^H\boldsymbol{S} \times \left[\boldsymbol{I}_{NN_t} + \frac{1}{4\sigma_w^2\sin^2\theta}\boldsymbol{L}\boldsymbol{S}\right]^{-1}\boldsymbol{\mu}\right) \times \left(\det\left[\boldsymbol{I}_{NN_t} + \frac{1}{4\sigma_w^2\sin^2\theta}\boldsymbol{L}\boldsymbol{S}\right]\right)^{-1} d\theta \tag{34}$$

where $\boldsymbol{S} = \boldsymbol{I}_N \otimes (\hat{\boldsymbol{s}} - \boldsymbol{s})(\hat{\boldsymbol{s}} - \boldsymbol{s})^H$ and $\boldsymbol{s} = [\boldsymbol{e}_{s_1}^T, \boldsymbol{e}_{s_2}^T, \cdots, \boldsymbol{e}_{s_K}^T]^T$.

By contrast, P_d in (32) is the BER of the APM symbols, under the assumption that all the spatial symbols are correctly detected. When the different APM schemes employed by AGrSM are taken into account, P_d can be evaluated from the formula [30]

$$P_d = \frac{1}{\eta_{APM}}\sum_{n=1}^{N_a}\left(\log_2 M_n\right)\bar{P}_b(n) \tag{35}$$

where $\bar{P}_b(n)$ is the average BER when the n-th modulation mode associated with a constellation size M_n is activated, which can be expressed as [41]

$$\bar{P}_b(n) = \int_{\gamma_n}^{\gamma_{n+1}} P_{b_n}(\gamma)f(\gamma)d\gamma. \tag{36}$$

Upon substituting $P_{b_n}(\gamma)$ and $f(\gamma)$ from (14) and (27) into the above equation and after some simplification [42], we obtain

$$\begin{aligned} \bar{P}_b(n) =& \frac{\left(\frac{NK}{r\bar{\gamma}_a}\right)^{\frac{N^2K^2}{r}}}{5\Gamma(\frac{N^2K^2}{r})}\int_{\gamma_n}^{\gamma_{n+1}}\gamma^{\frac{(NK)^2}{r}-1}\exp\left[-\lambda\gamma\right]d\gamma \\ =& \frac{\left(\frac{NK}{r\bar{\gamma}_a}\right)^{\frac{N^2K^2}{r}}}{5\Gamma(\frac{N^2K^2}{r})}\sum_{k=0}^{\lfloor (NK)^2/r-1\rfloor}\frac{\lfloor (NK)^2/r-1\rfloor!}{k!} \\ &\times\lambda^{-\frac{(NK)^2}{r}+k}\left[\gamma_n^k\exp(-\lambda\gamma_n) - \gamma_{n+1}^k\exp(-\lambda\gamma_{n+1})\right] \end{aligned} \tag{37}$$

where by definition, $\lambda = \frac{3}{2(M_n-1)} + \frac{NK}{r\bar{\gamma}_a}$.

5 Performance Results and Discussion

In this section, the performance of the proposed GrSM system is investigated and compared with some other similar schemes in the SM family, when assuming communications over correlated Rayleigh fading channels, or the correlated Rician fading channels with the parameter $\alpha = 5$ dB. Specifically, in the case of correlated Rician fading, the channel matrix can be rewritten as

$$\boldsymbol{H}_{\mathrm{r}} = \nu \boldsymbol{H}_{\mathrm{d}} + \sqrt{1-\nu^2}\boldsymbol{H} \tag{38}$$

where $\nu = \sqrt{\frac{\alpha}{\alpha+1}}$, and the LOS component of $\boldsymbol{H}_{\mathrm{d}}$ is assumed to satisfy $\mathrm{Tr}\left\{\boldsymbol{H}_{\mathrm{d}}\boldsymbol{H}_{\mathrm{d}}^{\mathrm{H}}\right\} = N \times N_g$. In our performance studies, the spatial correlation is modelled by the model in [26]. Both Monte-Carlo simulation and numerical evaluation of the expressions provided in the previous sections are considered.

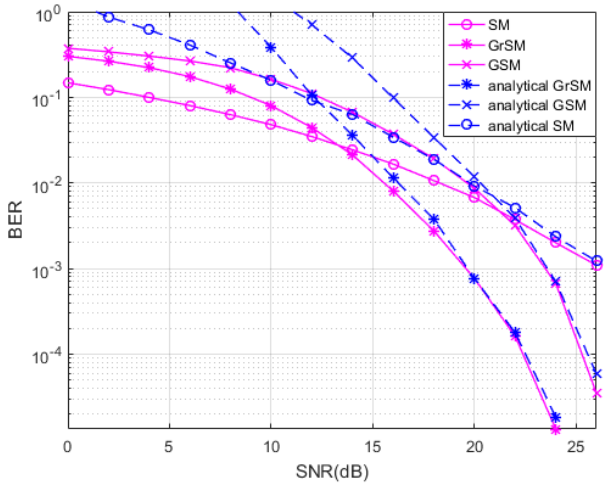

Fig. 1: BER versus SNR performance of the SM, GSM and GrSM schemes communicating over correlated Rician fading channels, when having the parameters $N_t = 16$, $N = 2$, $K = 2$, $\beta = 0.7$, $\eta = 8$ and $\alpha = 5$.

Fig. 1 depicts the BER versus SNR performance of the proposed GrSM system along with the SM and GSM systems, when the systems have the parameters $N_t = 16$, $N = 2$, $K = 2$, and $\beta = 0.7$. In order to provide a fair comparison, all the schemes are assumed to convey 8 bits per symbol. Then, it can be shown that for the GrSM, we have $N_g = 8$, and both the GrSM and GSM use the binary phase shift keying (BPSK) modulation. By contrast, the SM has to use 16-QAM. From the results of Fig. 1 we can observe that the analytical results converge to the simulation results as the SNR increases, and for all the schemes, the analytical results agree well with the simulation results, provided that the BER is about 10^{-3} or lower. At low SNR, as the spatial demodulation in the GrSM and GSM becomes less reliable due to multiple active antennas being used, the SM outperforms both the GrSM and GSM. By contrast, when the SNR is relatively high, resulting in that the spatial demodulation becomes sufficiently reliable, both the GrSM and GSM can outperform the SM arrangement, due to the fact that the BPSK employed by the GrSM and GSM is more reliable than the 16-QAM utilized by the SM. Furthermore, Fig. 1 shows that the GrSM always outperforms the GSM. This is because GrSM is capable of taking the antenna correlation into account, when the proposed antenna grouping is implemented.

In contrast to Fig. 1 concerning Rician channels, Fig. 2 shows the BER performance of the proposed GrSM as well as that of the conventional SM and GSM, when assuming communications over correlated Rayleigh fading channels. When compared with Fig. 1, we can surprisingly find that the performance of all the

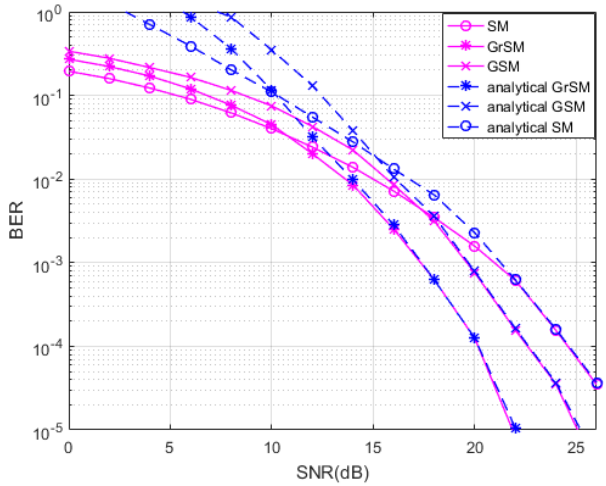

Fig. 2: BER versus the SNR performance of SM, GrSM and GSM systems communicating over correlated Rayleigh fading channels, when having the parameters $N_t = 16$, $N = 2$, $K = 2$, $\beta = 0.7$, and $\eta = 8$.

schemes over Rayleigh fading channels is respectively better than that of the schemes over Rician fading channels. This is because in Rician fading channels, the existence of LOS path yields a high spatial correlation both among the transmit antennas and among the receive antennas. This increased antenna correlation makes the spatial demodulation more difficult. In addition to the same observations as from Fig. 1, as shown in Fig. 2, at the BER of 10^{-5}, the performance gain achieved by the GrSM is about 3dB over the GSM scheme, and about 5dB when compared with the SM scheme.

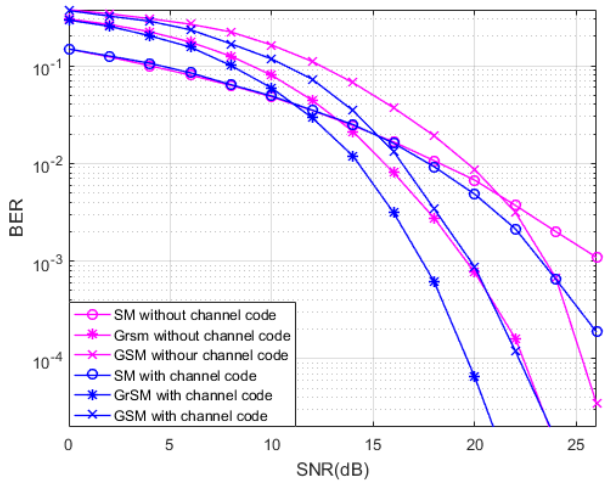

Fig. 3: BER versus SNR performance of SM, GrSM and GSM systems employing convolutional channel code, when communicating over correlated Rician fading channels and with the parameters $N_t = 16$, $N = 2$, $K = 2$, $\beta = 0.7$, $\eta = 8$ and $\alpha = 5$.

In Fig. 3 and Fig. 4, we investigate the effect of channel coding on the performance of different schemes, when Rician and Rayleigh fading channels are respectively considered. The system setup for Figs. 3 and 4 is exactly the same as that for Fig. 1. For channel coding, a rate $1/2$ convolutional code with the constraint length of $t = 3$ and the generators of 5 and 7 expressed in octal form are employed. Furthermore, interleaving between the first half of data with the last part of data is implemented to distribute the burst errors that may occur because of non-stationary channel noise. Explicitly, the results

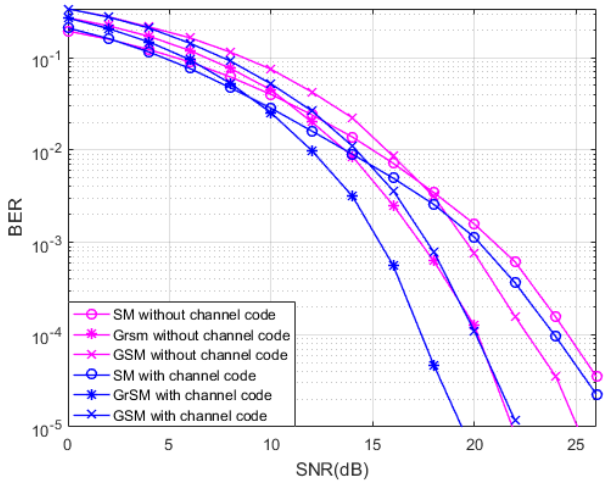

Fig. 4: BER versus SNR performance of SM, GrSM and GSM systems employing convolutional channel code, when communicating over correlated Rayleigh fading channels and with the parameters $N_t = 16$, $N = 2$, $K = 2$, $\beta = 0.7$ and $\eta = 8$.

in Figs. 3 and 4 demonstrate that the coded GrSM outperforms the coded GSM in both Rician and Rayleigh fading scenarios. Furthermore, the coded GrSM performs better than the coded SM in Rician fading channels provided that SNR$>$ 11 dB, and in Rayleigh fading channels provided that SNR$>$ 9dB. Moreover, with the channel coding, the BER performance of all the three schemes improved, and the improvement becomes significant, when SNR increases. Additionally, from Figs. 3 and 4, we can find that with the aid of channel coding, the intersection between the coded GrSM's BER curve and the coded SM's BER curve occurs about 2dB earlier than the intersection between the uncoded GrSM's BER curve and the uncoded SM's BER curve.

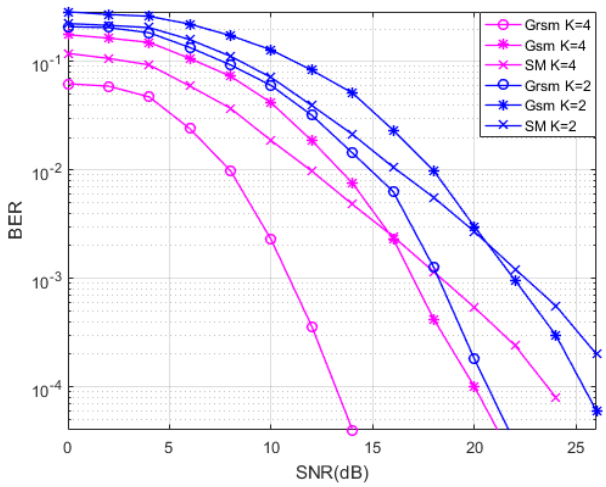

Fig. 5: BER versus SNR performance of SM, GrSM and GSM systems using different number of receive antennas, when communicating over correlated Rician fading channels and with the parameters of $N_t = 8, K = 4, \beta = 0.6, \eta = 10, \alpha = 5$.

In Figs. 5 and 6, the effect of the number of receive antennas on the BER performance of the three SM schemes is investigated. We assume the spectral efficiency of $\eta = 10$ bps/Hz, and the other parameters are detailed associated with the figures. The channel coding used is same as that for Fig. 3. To achieve $\eta = 10$ bps/Hz, we can readily figure out that GSM uses BPSK modulation for all active

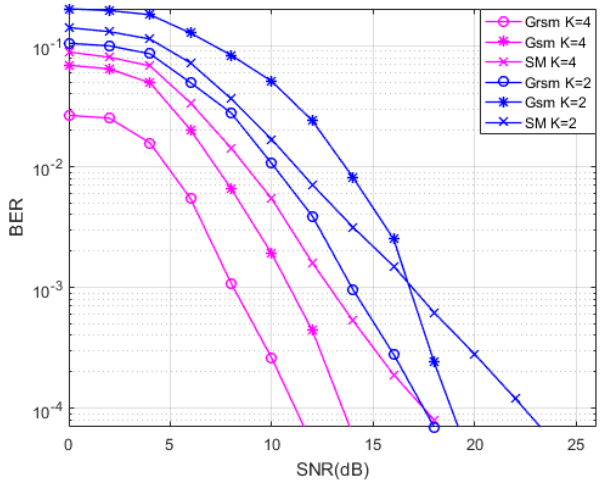

Fig. 6: BER versus SNR performance of SM, GrSM and GSM systems using different number of receive antennas, when communicating over correlated Rayleigh fading channels and with the parameters $N_t = 8, K = 4, \beta = 0.6, \eta = 10$.

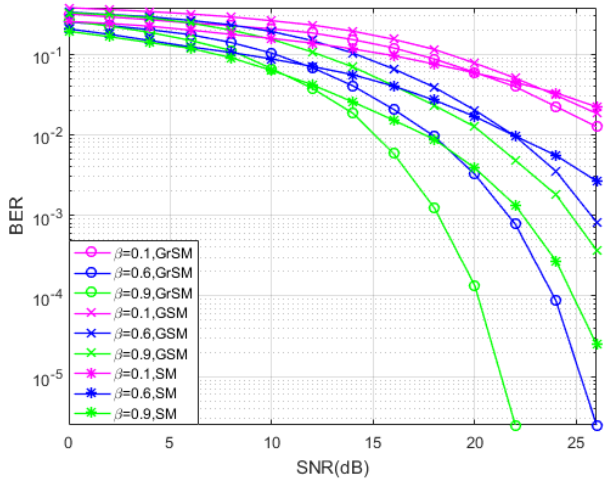

Fig. 7: Effect of channel correlation on the BER versus SNR performance of SM, GrSM and GSM systems over correlated Rician fading channels, and with the parameters $N_t = 16, K = 2, N = 2, \eta = 8, \alpha = 5$.

antennas, GrSM uses BPSK for two active antennas and 4-QAM for the other two active antennas, while SM has to use 128-QAM. From the results of Figs. 5 and 6 we observe that GrSM always outperforms the other two SM schemes. When under the Rician channels, the performance gain achieved by GrSM with $N = 2$ against GSM and SM is about 2dB and 4dB, respectively, at the BER of 10^{-4}. When $N = 4$, these gains become about 3 dB. By contrast, when communicating over Rayleigh fading channels and at the BER of 10^{-4}, as shown in Fig. 6, the performance gain achieved by GrSM with over GSM and SM is about 3dB and 4.5dB, respectively, when $N = 2$, and is about 2dB over both GSM and SM, when $N = 4$. The reason behind the above observation is that SM has a performance loss due to the employment of a high-order QAM, while GSM does not consider the antenna correlation, which degrades the achievable performance. As shown in Figs. 5 and 6, the BER performance of all three SM schemes improves with the increase of the number of receive antennas. When comparing the results in Fig. 6 (Rayleigh fading) with the corresponding ones in Fig. 5 (Rician fading), we can realize that the performance of all the three SM schemes degrades due to the LOS component of Rician fading channels.

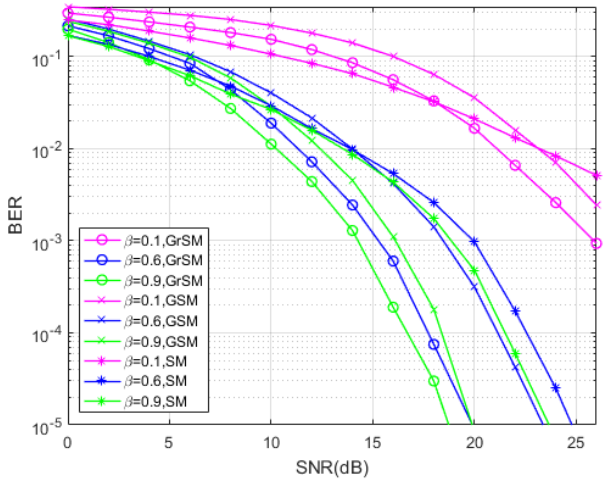

Fig. 8: Effect of channel correlation on the BER versus SNR performance of SM, GrSM and GSM systems over correlated Rayleigh fading channels, and with the parameters $N_t = 16, N = 2, K = 2, \eta = 8$.

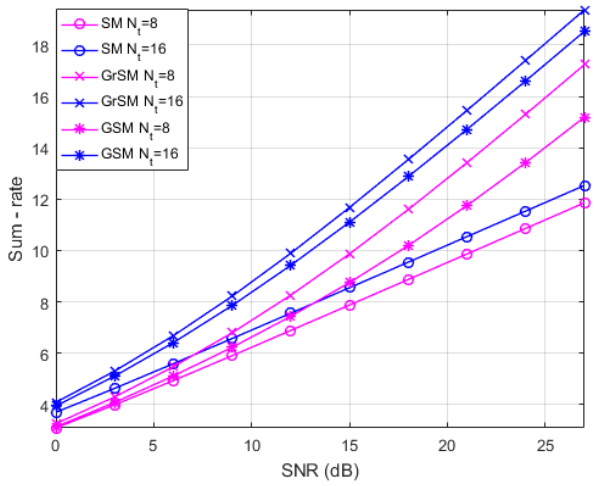

Fig. 9: Sum-rate achievable by the SM, GrSM and GSM systems over Rician fading channels with respect to $N_t = 8$ and $N_t = 16$, when the other parameters of $K = 2, N = 2, \beta = 0.6$, $\alpha = 5$ are assumed.

In order to investigate the impact of the channel correlation on the BER performance, in Figs. 7 and 8, we compare the BER performance of the three SM schemes over Rician (Fig. 7) and Rayleigh (Fig. 8) channels, when the correlation coefficient is set to $\beta = 0.1, 0.6$ and 0.9. As the correlation coefficient is given by $\gamma = \exp(-\beta)$, $\beta = 0.1, 0.6$ and 0.9 correspond to strong, medium and weak correlation. Furthermore, in our simulation, the parameters are detailed in the figures, while the channel code employed by the three schemes is the same as that for Fig. 3. From the results of Figs. 7 and 8, we observe that the BER performance of all three SM schemes degrades, when the channel correlation becomes stronger. This is because the increase of correlation results in the increase of spatial interference. When comparing the BER performance of the three SM scheme, we can see that the proposed GrSM always outperform the other two SM schemes, provided that the SNR is in the desired range, resulting in that the BER is below 10^{-2}. When SNR is small, there may exist intersection between GrSM and SM's BER curves, when β is large. Again, the BER performance over Rayleigh fading channels is better than the corresponding BER performance over Rician fading channels.

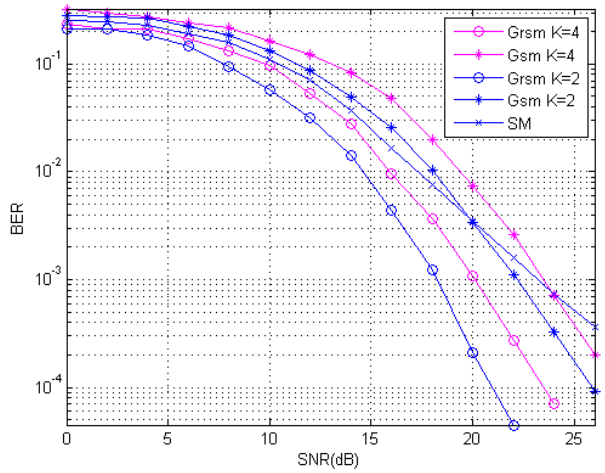

Fig. 10: BER versus SNR performance of SM, GrSM and GSM systems over correlated Rician fading channel, and with the parameters $N_t = 8, K = 2/4, N = 2, \eta = 10, \alpha = 5, \beta = 0.6$.

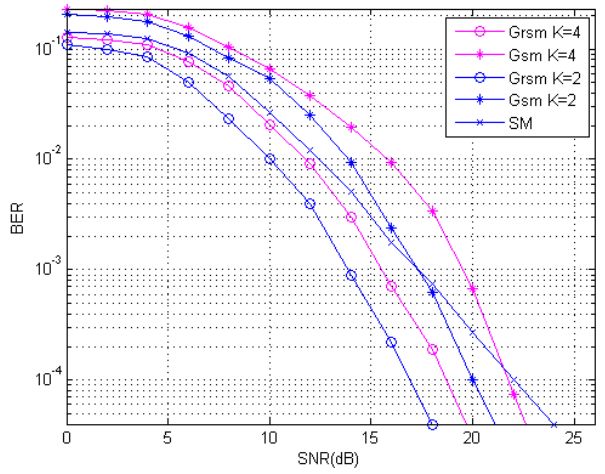

Fig. 11: BER versus SNR performance of SM, GrSM and GSM systems over correlated Rayleigh fading channel with $N_t = 8, K = 2/4, N = 2, \eta = 10, \beta = 0.6$.

Fig. 9 demonstrates the achievable sum-rates of the GrSM, GSM and SM schemes with the parameters listed in the caption, when communicating over Rician fading channels. For a given SNR, the proposed GrSM always achieves the highest sum-rate among the three SM schemes, as the result that GrSM is designed with taking antenna correlation into account. When the number of transmit antennas increases, explicitly, the sum-rate of all the SM schemes increases, with the increase of GSM's sum-rate most significantly.

The effect of the number of groups K for a given number of transmit antennas on the BER performance of SM, GSM and proposed GrSM is shown in Fig. 10 over Rician fading channels and in Fig. 11 over Rayleigh fading channels. Note that, the channel coding used in our simulations was the same as that for Fig. 3, and the settings for baseband modulation schemes were the same as that for Fig. 5. As shown in Fig. 10, at the BER of 10^{-4}, GrSM has 3.5dB performance gain over GSM when $K = 2$, and has 2dB performance gain over GSM when $K = 4$. For GrSM, the BER performance with $K = 2$ outperforms that with $K = 4$. By contrast, the GSM with $K = 4$ outperforms the GSM with $K = 2$. Similar observations can also be derived from Fig. 11 considering Rayleigh fading, except that the relative performance gains have slight differences. From the results of Figs. 10 and 11 we can conceive that when given the channel, data

rate, and the number of transmit/receive antennas, there is an optimum number of groups for the GrSM (or GSM) to achieve the best BER performance.

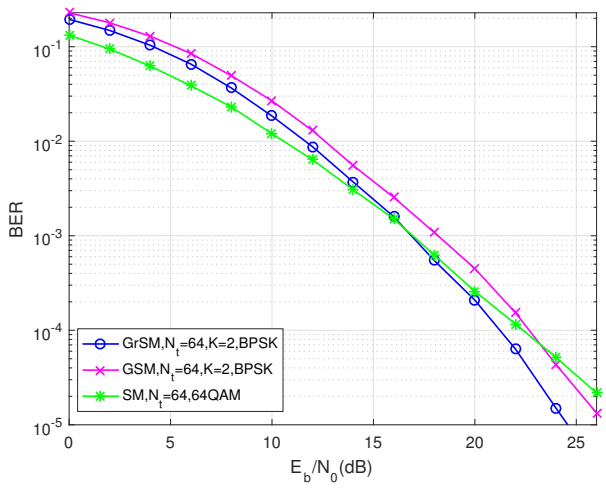

(a) $N_t = 64$

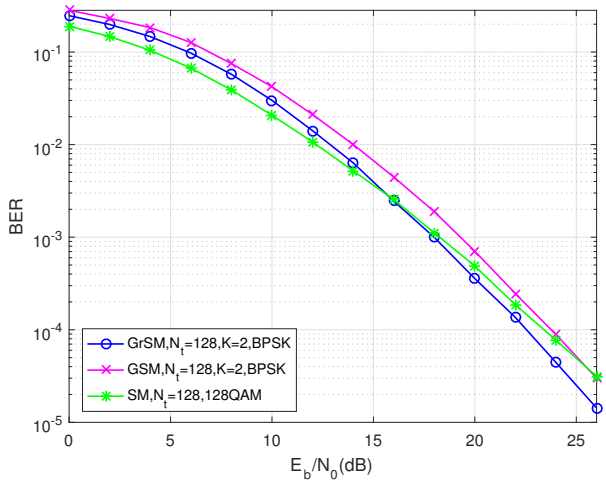

(b) $N_t = 128$

Fig. 12: BER versus SNR performance of SM, GrSM and GSM systems communicating over correlated Rician fading channels, with $K = 2, N = 2, \beta = 0.6$, and $N_t = 64$ or 128.

In Fig. 12, we compare the BER performance of the GrSM, SM and GSM communicating over Rician fading channels, when $N_t = 64$, or 128 transmit antennas, and the other parameters of $K = 2, N = 2, \beta = 0.7$ are used. In our studies, the channel coding scheme used with Fig. 12 is same as that used for the previous figures. Note furthermore that to achieve $\eta = 12$ bps/Hz, the GrSM and GSM with $N_t = 64$ can use BPSK modulation, while the corresponding SM has to use $64-$QAM. When $N_t = 128$, we set $\eta = 14$ bps/Hz. In this case, BPSK modulation is employed by both the GrSM and GSM schemes, while the SM has to use $128-$QAM. As shown in Fig. 12, GrSM outperforms both GSM and SM in relatively high SNR region, while in low to medium SNR region, the BER performance of GrSM falls between that of SM and that of GSM.

In Fig. 13 we investigate the BER versus SNR performance of the proposed AGrSM and the AGSM systems, when assuming communications over correlated Rayleigh fading channels. In our simulations, the modulation schemes employed include $4-$QAM, 8-PSK, 16-QAM and $32-$QAM, and the systems have the parameters

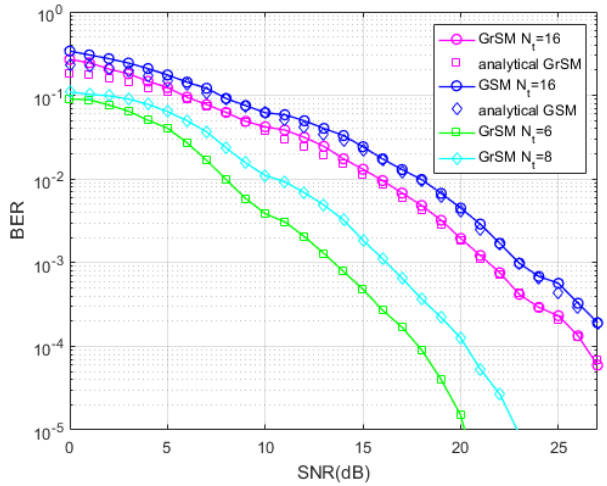

Fig. 13: BER versus SNR performance of AGrSM and AGSM systems communicating over correlated Rayleigh fading channels, when $K = 2, N = 2, \beta = 0.6$ and $N_t = 16$.

of $N_t = 16, \beta = 0.7$, and $N = 2$, $K = 2$, while the target BER is 10^{-3}. Furthermore, GrSM and GSM with $4-$QAM and $32-$QAM are also shown in Fig. 13 for comparison. In Fig. 13, the numerical results evaluated from our analytical expressions are also provided, which are shown to be the lower bound of the simulation results. In comparison with the previous figures, the BER of both the AGrSM and the AGSM is changed and becomes flatter with the increase of SNR. This is the result of the increase of data rate, as the SNR increases. However, when the SNR is high enough to use the highest modulation level of 32-QAM, the BER then decreases towards zero, if SNR further increases. As shown in Fig. 13, AGrSM always has better performance than AGSM for any given constellation size.

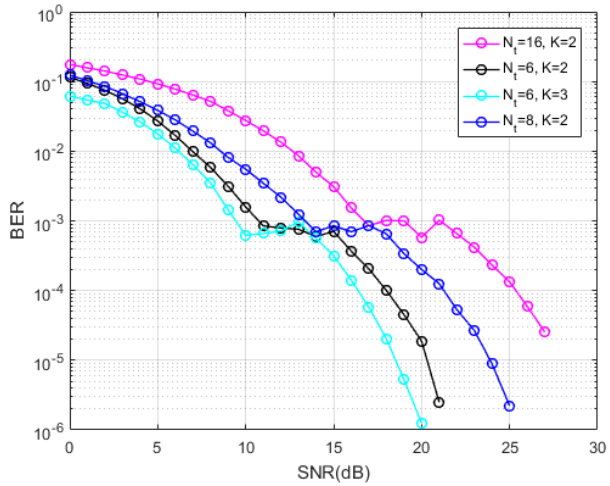

Fig. 14: BER versus SNR performance of the AGrSM systems communicating over correlated Rayleigh fading channels, when $K = 2, N = 2, \beta = 0.6$, and when N_t takes various values.

Fig. 14 shows the BER versus SNR performance of the proposed AGrSM systems with different number of transmit antennas, when the target BER P_{b_0} is assumed to be 10^{-3}. In our studies, the correlation coefficient of transmit antennas is chosen to be $\beta = 0.6$ to count a moderate correlation. Explicitly, increasing the number of transmit antennas leads to a higher spectral efficiency, as shown in Fig. 15, whereas degrades the BER performance of AGrSM. This is

because, when communicating at a higher rate by using more transmit antennas, the erroneous detection of antenna indices occurs more frequently. In this case, the maximum likelihood (ML) detection also leads to a higher probability of erroneous detection of the constellation symbols. Consequently, the overall BER performance degrades, as the number of transmit antennas increases and when the AGrSM system supports the data rate as shown in Fig. 15.

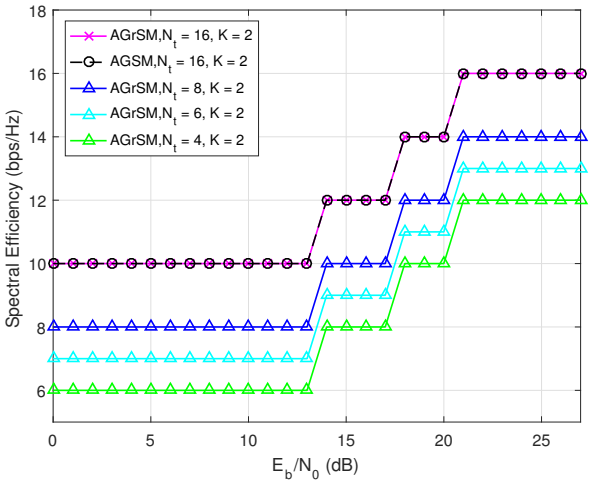

Fig. 15: Spectral efficiency versus SNR performance of AGrSM and AGSM systems communicating over correlated Rayleigh fading channels, with $K = 2, N = 2, \beta = 0.6$ and N_t taking different values.

Finally, the spectral efficiency versus SNR performance of the AGrSM and AGSM systems with respect to different number of transmit antennas is depicted in Fig. 15. As shown in Fig. 15, when $N_t = 16$, both AGrSM and AGSM achieve the same spectral efficiency, while the BER performance of AGrSM outperforms that of AGSM, as shown in Fig. 13. Furthermore, when jointly observing the BER and spectral efficiency performance, as shown in Fig. 14 and Fig. 15, respectively, We can conceive that there is a trade-off between spectral efficiency and BER performance. While the case of $N_t = 16$ achieves the highest spectral efficiency for a given SNR, as shown in Fig. 15, it also results in the worst BER performance, as shown in Fig. 14. By contrast, while the case of $N_t = 8$ achieves a higher spectral efficiency than the case of $N_t = 6$, it also has a better BER performance than the case of $N_t = 6$.

6 Conclusion

In this paper, we have proposed a GrSM scheme for supporting massive MIMO communications with correlated antennas. The effect of antenna correlation is mitigated by grouping the strongly correlated antennas into the same group to support spatial modulation, while the weakly correlated antennas are assigned to different groups to benefit for achieving multiplexing gain. AM has been introduced to the GrSM in order to improve the spectral efficiency. We have theoretically analysed the achievable BER and spectral efficiency of GrSM and AGrSM systems. The BER and spectral efficiency performance of GrSM and AGrSM systems have been investigated with the aid of both Monte Carlo simulations and numerical evaluation of the analytical expressions, showing that our analytical results are valid for BER and spectral efficiency prediction. Furthermore, the performance of GrSM (AGrSM) has been compared with that of SM (ASM) and of GSM (AGSM), when various communication scenarios are considered. Our studies demonstrate that, aided by our proposed antenna grouping strategy, the BER or spectral efficiency performance of GrSM (AGrSM) are capable of outperforming that of SM (ASM) and GSM (AGSM). For given wireless channel, the number of transmit/receive antennas, and the data rate, there exists an optimum number of groups yielding the best BER performance. Additionally, under these conditions, the number of bits conveyed by spatial modulation and that by APM can be appropriately chosen for attaining the best possible BER performance. Our future work may include the adaptive antenna grouping based on compressed CSI for the frequency-division duplexing massive MIMO, as well as seeking the effective approaches to derive the optimum number of groups and the optimum number of active antennas that yield the best BER performance.

Acknowledgement

The financial support of the National Natural Science Foundation of China (NSFC): 61571401, 61271421, 61301150 and the Innovative Talent of Colleges and University of Henan Province under grant 18HASTIT021 are gratefully acknowledged. The last author would like to acknowledge the financial support of the EPSRC project EP/P034284/1.

7 References

1 Wen, M., Zheng, B., Kim, K.J., Di.Renzo, M., Tsiftsis, T.A., Chen, K.C., et al.: 'A survey on spatial modulation in emerging wireless systems: Research progresses and applications', *IEEE Journal on Selected Areas in Communications*, 2019, **37**, (9), pp. 1949–1972

2 He, L., Wang, J., Song, J.: 'Spatial modulation for more spatial multiplexing: RF-chain-limited generalized spatial modulation aided MM-Wave MIMO with hybrid precoding', *IEEE Transactions on Communications*, 2017, **66**, (3), pp. 986–998

3 Zhang, P., Chen, J., Yang, X., Ma, N., Zhang, Z.: 'Recent research on massive MIMO propagation channels: A survey', *IEEE Communications Magazine*, 2018, **56**, (12), pp. 22–29

4 Zhang, J., Zhang, B., Chen, S., Mu, X., El.Hajjar, M., Hanzo, L.: 'Pilot contamination elimination for large-scale multiple-antenna aided OFDM systems', *IEEE Journal of Selected Topics in Signal Processing*, 2014, **8**, (5), pp. 759–772

5 Li, Y., Lei, X., Tang, W., He, D., Xiao, Y., Xiang, W.: 'Performance analysis of MMSE pre-coding aided spatial modulation', *IEEE Access*, 2018, **6**, pp. 44835–44845

6 Hussein, H.S., Elsayed, M., Mohamed, U.S., Esmaiel, H., Mohamed, E.M.: 'Spectral efficient spatial modulation techniques', *IEEE Access*, 2019, **7**, pp. 1454–1469

7 Renzo, M.D., Haas, H., Ghrayeb, A., Sugiura, S., Hanzo, L.: 'Spatial modulation for generalized MIMO: challenges, opportunities, and implementation', *Proceedings of the IEEE*, 2014, **102**, (1), pp. 56–103

8 Xiao, L., Xiao, P., Xiao, Y., Wu, C., Nguyen, H.V., Hemadeh, I.A., et al.: 'Transmit antenna combination optimization for generalized spatial modulation systems', *IEEE Access*, 2018, **6**, pp. 41866–41882

9 Narasimhan, T.L., Raviteja, P., Chockalingam, A.: 'Generalized spatial modulation in large-scale multiuser MIMO systems', *IEEE Transactions on Wireless Communications*, 2015, **14**, (7), pp. 3764–3779

10 Younis, A., Serafimovski, N., Mesleh, R., Haas, H. 'Generalised spatial modulation'. In:2010 Conference Record of the Forty Fourth Asilomar Conference on Signals, Systems and Computers. Pacific Grove, CA, USA, Nov., 2010. pp. 1498–1502

11 Narasimhan, R.: 'Spatial multiplexing with transmit antenna and constellation selection for correlated MIMO fading channels', *IEEE Transactions on Signal Processing*, 2003, **51**, (11), pp. 2829–2838

12 Ishikawa, N., Rajashekar, R., Xu, C., El-Hajjar, M., Sugiura, S., Yang, L., et al.: 'Differential-detection aided large-scale generalized spatial modulation is capable of operating in high-mobility millimeter-wave channels', *IEEE Journal of Selected Topics in Signal Processing*, 2019, pp. 1–1

13 Kim, K., Ko, K., Lee, J. 'Mode selection between antenna grouping and beamforming for MIMO communication systems'. In: 43rd Annual Conference on Information Sciences and Systems (CISS). Baltimore, MD, USA, June 2009. pp. 506–511

14 Lee, B.M.: 'Energy efficient selected mapping schemes based on antenna grouping for industrial massive mimo-ofdm antenna systems', *IEEE Transactions on Industrial Informatics*, 2018, **14**, (11), pp. 4804–4814

15 Rajashekar, R., Yang, L., Hari, K.V.S., Hanzo, L.: 'Transmit antenna subset selection in generalized spatial modulation systems', *IEEE Transactions on Vehicular Technology*, 2019, **68**, (2), pp. 1979–1983

16 Kim, K., Lee, J., Liu, H.: 'Spatial-correlation-based antenna grouping for MIMO systems', *IEEE Transactions on Vehicular Technology*, 2010, **59**, (6), pp. 2898–2905

17 Ju, P., Zhang, M., Cheng, X., Wang, C.X. 'Generalized spatial modulation with transmit antenna grouping for correlated channels'. In: IEEE International Conference on Communications. Kuala Lumpur, Malaysia, July 2016. pp. 1–6

18 Khederzadeh, R., Farrokhi, H.: 'Adaptive rate and power transmission in spectrum-sharing systems with statistical interference constraint', *IET Communications*, 2014, **8**, (6), pp. 870–877

19 Hassan, Z., Hossain, J., Cheng, J., Leung, V.C.: 'Delay-qos-aware adaptive modulation and power allocation for dual-channel coherent owc', *IEEE/OSA Journal of Optical Communications and Networking*, 2018, **10**, (3), pp. 138–151

20 Abdelaziz, M., Gulliver, T.A.: 'Triangular constellations for adaptive modulation', *IEEE Transactions on Communications*, 2018, **66**, (2), pp. 756–766
21 Bouida, Z., Ghrayeb, A., Qaraqe, K.A. 'Adaptive spatial modulation for spectrally-efficient MIMO spectrum sharing systems'. In: IEEE 25th Annual International Symposium on Personal, Indoor, and Mobile Radio Communication. Washington, DC, USA, June 2014. pp. 354–358
22 Afridi, S., Hassan, S.A. 'Spectrally efficient adaptive generalized spatial modulation MIMO systems'. In: 14th IEEE Annual Consumer Communications and Networking Conference. Las Vegas, NV, USA, July 2017. pp. 260–263
23 Larsson, E.G., Edfors, O., Tufvesson, F., Marzetta, T.L.: 'Massive MIMO for next generation wireless systems', *IEEE Communications Magazine*, 2014, **52**, (2), pp. 186–195
24 Qu, W., Zhang, M., Cheng, X., Ju, P.: 'Generalized spatial modulation with transmit antenna grouping for massive MIMO', *IEEE Access*, 2017, **5**, (2017), pp. 26798 – 26807
25 Zelst, A.V., Hammerschmidt, J.S.: 'A single coefficient spatial correlation model for multiple-input multiple-output (MIMO) radio channels', *in 27th General Assembly of the International Union of Radio Science (URSI), Maastricht, The Netherlands*, Aug. 17-24,2002, pp. 1–4
26 Martin, C., Ottersten, B.: 'Asymptotic eigenvalue distributions and capacity for MIMO channels under correlated fading', *IEEE Transactions on Wireless Communications*, 2004, **3**, (4), pp. 1350–1359
27 Yang, Y., Jiao, B.: 'Information-guided channel-hopping for high data rate wireless communication', *IEEE Communications Letters*, 2008, **12**, (4), pp. 225–227
28 Yang, L.L.: 'Multicarrier communications'. (John Wiley & Sons, 2009)
29 Telatar, I. E.: 'Capacity of multiantenna Gaussian channels', *European Transactions on Telecommunications*, 1999, **10**, (6), pp. 585-595.
30 Alouini, M.S., Goldsmith, A.J.: 'Adaptive modulation over Nakagami fading channels', *Wireless Personal Communications*, 2000, **13**, (1-2), pp. 119–143
31 Wu, X., Renzo, M.D., Haas, H.: 'Adaptive selection of antennas for optimum transmission in spatial modulation', *IEEE Transactions on Wireless Communications*, 2015, **14**, (7), pp. 3630–3641
32 Proakis, J.G.: 'Digital Communications'. 5th ed. (McGraw Hill, 2007)
33 Alouini, M.S., Goldsmith, A.J.: 'A unified approach for calculating error rates of linearly modulated signals over generalized fading channels', *IEEE Transactions on Communications*, 1999, **47**, (9), pp. 1324–1334
34 Savage, I.R.: 'Millą́s ratio for multivariate normal distributions', *Journal of Research of the National Bureau of Standards*, 1962, **66B**, (3)
35 Liu, Y., Yang, L., Hanzo, L.: 'Spatial modulation aided sparse code-division multiple access', *IEEE Transactions on Wireless Communications*, 2018, **17**, (3), pp. 1474–1487
36 Pan, P., Yang, L.: 'Spatially modulated code-division multiple-access for high-connectivity multiple access', *IEEE Transactions on Wireless Communications*, 2019, **18**, (8), pp. 4031–4046
37 Wypych, G.: 'Principles of statistics'. (Dover Publications,, 1979)
38 Torabi, M., Nerguizian, C.: 'Impact of antenna correlation on the BER performance of a cognitive radio network with Alamouti STBC', *IEEE Wireless Commun Letters*, 2016, **5**, (3), pp. 264–267
39 Mesleh, R.Y., Haas, H., Sinanovic, S., Chang, W.A., Yun, S.: 'Spatial modulation', *IEEE Transactions on Vehicular Technology*, 2008, **57**, (4), pp. 2228–2241
40 Naidoo, N.R., Xu, H.J., Quazi, A.M.: 'Spatial modulation: optimal detector asymptotic performance and multiple-stage detection', *IET Communications*, 2011, **5**, (10), pp. 1368–1376
41 Goldsmith, A.J., Chua, S.G.: 'Variable-rate variable-power mqam for fading channels', *IEEE transactions on communications*, 1997, **45**, (10), pp. 1218–1230
42 Gradshteyn, I.S., Ryzhik, I.M.: 'Table of integrals, series, and products'. (Academic press, 2014)